Effect of dry deposited particles on the tire/road friction

Yosra Hichri, Véronique Cerezo, Minh Tan Do

Effect of dry deposited particles on the tire/road friction

Y. Hichri*, V. Cerezo, M. T. Do

IFSTTAR, AME-EASE, 44344 Bouguenais, France.

.

* Corresponding author

Address: IFSTTAR, Route de Bouaye, CS4, 44344, Bouguenais Cedex

Email: yosra.hichri@ifsttar.fr

Abstract

Road accidents increase during the first rain after a long dry period. It is widely accepted that the tire traction loss is due to fine particles accumulated on the road surface. Yet, the involved mechanisms at the tire/road interface are not clearly understood.

This paper deals with the particle-induced lubrication on dry road. Tests are performed in laboratory. Sediments are extracted from a catchment area which collects runoff water. The process of extracting particles from sediments in laboratory by drying and sieving is described. Particles are separated into fractions characterized by their chemical composition and size distribution. Protocol to simulate the process of particles' build-up on the road surface is described. The effect of the particle's size and concentration is studied. Surfaces representative of real road surface textures are tested. Friction tests are conducted using the Skid Resistance Tester, which is widely used to assess friction characteristics of road surfaces. Samples are weighed before and after each friction run. On a surface initially covered by a compacted particle layer, successive friction runs are performed, without resupplying particles, to follow the evolution of the friction coefficient with the particle depletion.

Friction drops significantly when a surface is covered by particles. Successive runs induce an increase of the friction coefficient until reaching a stable value which is still lower than that of a clean surface. Particles are considered as third bodies introduced artificially in the interface between the friction slider and the test sample. Analysis of particles' flows (particles trapped and ejected), through particles' mass extracted from weighing, helps to explain the friction variation.

Assuming that friction is governed by the surface fraction (X) covered by particles, a model was developed. The calculated friction coefficient is a weighted sum of friction coefficients when the surface is respectively

clean (X = 0) and fully covered by particles (X = 1). It was found that the surface fraction can be expressed as a function of the ratio of available particles' mass to initial particles' mass. Comparisons between model and experiment are satisfactory. Discussions are made in terms of interactions between surface textures and particles' size and concentration.

Keywords: friction, particles, dry lubrication, mass of particles, index of starvation.

1. Introduction

Road accidents increase during the first rain after a long dry period [1]. Eisenberg [1] analyzed the relationship between precipitation and traffic crashes over 25 years in the US and found a significantly increasing crash risk with the number of dry days since the last rain. This excess risk is generally attributed to the accumulation of fine particles on the road surface. The origin of these particles is diverse (dust, debris from tires, road surface and equipment, etc.). Authors in [2][3] developed models to predict the particle's accumulation, also known as particle's build-up, as a function of the number of dry days and other weather conditions such as wind characteristics, traffic, etc. The same authors looked also at the particle size distribution depending on the land use (industrial, residential, commercial, etc.). For example, Egodawatta [3] observed the distribution of the particles' size in three urban areas and found that 50% (resp. 70%) of the particles are less than 100 µm (resp. 200 µm) in size. On highways surfaces, Shakely et al. [4] collected particles by vacuum cleaner and found mainly particles bigger than 50 µm followed by the fractions 7-50 µm and 3.3-7 µm.

Shakely et al. [4] found on the other hand that friction coefficient, measured by a locked wheel (full sliding) equipped with rubber tire, decreases with increasing dust concentration. Wilson [5] showed a graph illustrating how friction varies over a dry-wet-dry period. The friction coefficient is considered as constant during the dry period; at the first rain drops, friction coefficient decreases significantly; as the rain continues to fall, the surface is washed and friction coefficient increases until reaching a stable value; as the rain stops and the surface dries, it increases to a level similar to that prior to the rain. Do et al. [6] developed in laboratory an experimental protocol which reproduces qualitatively the loss of skid resistance with time during a rain preceded by a long dry period. These authors investigated the effect of particles' concentration and found that higher concentrations induce lower friction coefficients and delay the washing process. Visual observations of the road samples showed that residual contaminants can still be observed even after the wash-off period.

It can be said that the risk induced by fine particles on road safety is well perceived. However, the way these particles act on the tire/road friction is still questionable. In the road field, dry friction is most of the time considered as satisfactory and water is usually designated as the main element which is harmful for drivers. Actually, when the road surface is wet, there is a sharp reduction in the friction coefficient due to the presence of a water film acting as a lubricant between the tire and the road surface. Kulakowski and Harwood [7] reported that even a water depth as thin as 0.025mm on the road can reduce the tire/road friction by as much as 75% compared with a dry surface. Do et al. [8] found on the other hand that, depending on the surface microtexture (asperities provided by road aggregates), wet friction coefficient can be maintained at a value near to the dry friction coefficient until a critical water depth is reached. Relationship was found between the critical water depth and the asperities' height [8]. Sabey [9] conducted friction tests with spherical and conical single sliders and proved that there is a link between the calculated average pressure exerted by the sliders (on an elastic plane) and the measured wet friction coefficient (between the sliders and a rubber plane). Savkoor [10] explained Sabey's findings by the fact that the water depth at the asperities' summits can be as low as 10μm and only a high pressure exerted by sharp asperities can break the water film and reestablish direct contact between the tire and the road.

The presence of particles on the road is considered as an additional element which degrades the wet friction. Lambourn and Viner [11] tested various contaminants (clay, sand, etc.) on road surfaces and found a substantial decrease of the friction coefficient (divided by 2) when the surface is contaminated compared with the dry friction coefficient. Persson [12] said that the mix of particles with water is highly viscous and then lubricates more the tire/road interface. The lubricating action of particles mixed with lubricants has been observed in other tribosystems like piston ring-cylinder liner pairs in internal combustion engines [13][14][15]. These authors have shown that adding additives like molybdenum disulfide [13][14] or graphite [15] in oils helps to reduce friction and wear. Xu and coauthors in [15] attributed this performance to the higher viscosity of oil with additives (an esterified bio-oil has been used) compared with pure oil. This observation corroborates that made by Persson in [12].

However, other authors found that the particles alone can induce lubrication actions. Li et al. [16] studied the friction between footwear and floor covered with particles and found that particles can reduce the friction coefficient even under dry conditions. According to these authors, the dry friction coefficient decreases when the particles' size increases. Mills et al. [17], who also studied friction on dry floors covered by particulate contaminants, stated that there is a critical size of the particles (around 50-60 μm) above which particles roll one

on the other, when a rubber pad slides on the floor, and below which they tend to stick together due to cohesive forces and promote a sliding mechanism at the rubber slider/floor interface. On the other hand, the roughness of the floor's surface can trap a proportion of particles and, by preventing particles passing over the surface asperities, contributes to the shearing of the particle layer [17]. Heshmat [18] has demonstrated that solid particles can form load-carrying lubricant films which exhibit a behavior resembling that of fluid films. This author looked at full particles' film whereas other authors, like Higgs et al. [19], studied the case of partially covered surfaces. Regardless of the lubrication regime, authors agree that triboparticulates – to reuse a definition provided by Blau in [20] – have an effect on friction between two contacting bodies. So logically particles deposited on road surfaces should have an effect on the tire/road friction under dry condition as well.

To fully understand the effect of deposited particles on tire/road friction, there is then a need to investigate the dry road condition. This paper presents a laboratory study aiming at contributing to this objective. Friction tests are performed to assess the effect of particles' size and concentrations which are known as factors affecting the particle's build-up during a dry period [3]. Analyses are performed to represent friction variation and explain it by the particles' flows. A model is proposed to represent experimental data and helps to get some insights into the involved mechanisms.

2. Research methodology

Friction analysis provides valuable information about the effect of particles on road skid resistance. However, understanding the lubrication mechanisms needs another approach much more directly linked to the particle itself. We have thought that using the third body concept, as developed originally by Godet [21], could be a relevant way to reach this aim. Godet considered that two-body contacts merely exist only during the very first moment of rubbing and third bodies are generated practically immediately; the consequence is that a two-body contact is most of the time a mixed contact. Third-bodies can be lubricants, such as oils or powder, or debris detached – due to wear – from the first bodies. They can have a lubrication action or a load-carrying role. Godet stated that to fully predict load and friction in contacts with a third body at the interface, at least three conditions are required: the knowledge of the rheological behavior of the third-body material, information about boundary conditions (for example, how particles adhere or roll on the face of the first bodies), and the existence of a general theory of thin film mechanics. As the nature of third bodies is very diverse, as well as the way they circulate inside the contact, prediction tools must be adapted to specific materials and operating conditions.

In the present study, the third body – particles – is artificially introduced into the tire/road contact, even if

some natural third bodies can exist too. A weighing procedure is developed to extract the mass of particles before and after friction measurements. Friction and particles' mass are analyzed separately then combined to see how particles govern friction. The analysis presented in the following paragraphs has been inspired from works of Fillot et al. [22]. These authors studied wear-induced particles. Using a mass equilibrium equation and expressing separately the particle detachment (source) flow and the particle ejection (wear) flow, they developed an analytical model based on particles' masses to explain wear as a competition between the source and wear flows. Even if Fillot and coauthors focused their analysis on wear, many similarities exist between the wear particles' flows and the flows of particles investigated in the present paper. We have thought that analyzing particles' flows inside the contact using particles' masses would be promising to understand how the particles behave at the rubber slider/test sample interface (formation of interfacial layer, ejection, etc.).

In the modeling phase, we had looked for a model expressing the fact that the rubber slider (which represents a tire tread element) is supported partly by the particles' layer and partly by direct contact between the slider and the surface asperities. The objective is to dispose of a physical model whose parameters can be related to the particles' characteristics.

3. Experimental program

3.1. Test sample

Test sample is an aluminum rectangular slab of 130mm × 80mm × 15mm (surface of 130mm × 80 mm ≈ 0.01m^2). The slab dimensions are required by the device used for friction measurements. The choice of aluminum to represent a road surface can seem to be surprising. Actually, the test protocol requires weighing of the test sample before and after friction measurements to determine the flow of particles at the rubber slider/test sample interface and road samples are too heavy for the precision scale used in the study. Different surface treatments were then sought to reproduce a surface roughness similar to that of road surface microtexture (surface irregularities whose dimensions are below 0.5 mm horizontally and vertically). The microtexture scale is studied because it is responsible for the generation of frictions forces [23] and is masked by deposited particles [5]. The most relevant method consists in sandblasting the aluminum surface using corundum particles whose size characteristics are shown in table 1. It was found that sandblasting can create a texture comparable to that of a road aggregate (Fig. 1).

Tab.1 Size characteristics of corundum particles

Sieving (mm)	Passing (%)
2.00	100
1.00	90-100
0.710	30-40
0.500	0-15
0.400	0-5
0.250	0-5

a) 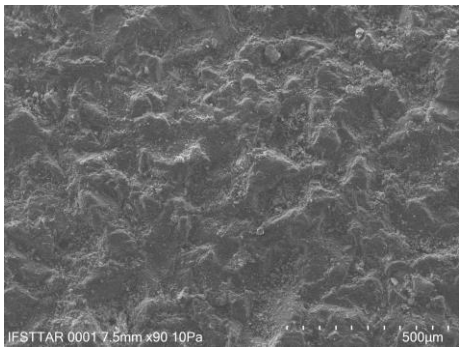

b) 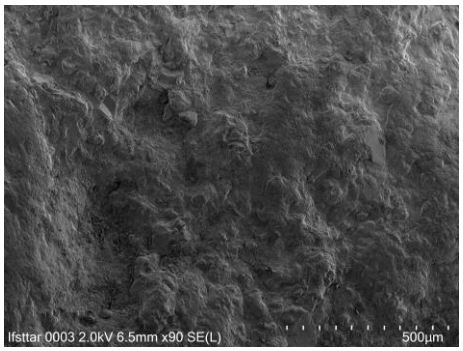

Fig.1 Surfaces of (a) the sandblasted aluminum sample and (b) an aggregate viewed by SEM

Roughness parameters derived from ISO 25178-2 [24] are used to characterize the test samples and compare their texture to that of a road aggregate (limestone) (Tab. 2). It can be seen that the roughness of the sandblasted aluminum is similar to that of an aggregate polished by the traffic. Details of the 3D cartography measurement are given in the test procedure (section 3.5).

Tab.2 Surfaces roughness parameters

Parameter	Aggregate		Aluminum sample
	Unpolished	Polished	
S_q (µm) (root mean square height)	39.4	16.8	13.9
V_{mp} (ml/m^2) (peak material volume)	1.88	0.702	0.604
V_{mc} (ml/m^2) (core material volume)	30.7	12.8	12.3
V_{vc} (ml/m^2) (core void volume)	43.3	17.9	15.7
V_{vv} (ml/m^2) (valley void volume)	5.42	2.38	1.82

3.2. Particles collecting and characterization

Particles are collected at the catchment area of Cheviré near Nantes. This area collects runoff water coming from the South part of the Cheviré bridge (Fig. 2). This bridge of more than 1.5 km in length crosses the Loire river and supports a daily traffic of 90,000 vehicles with 8.5% of trucks.

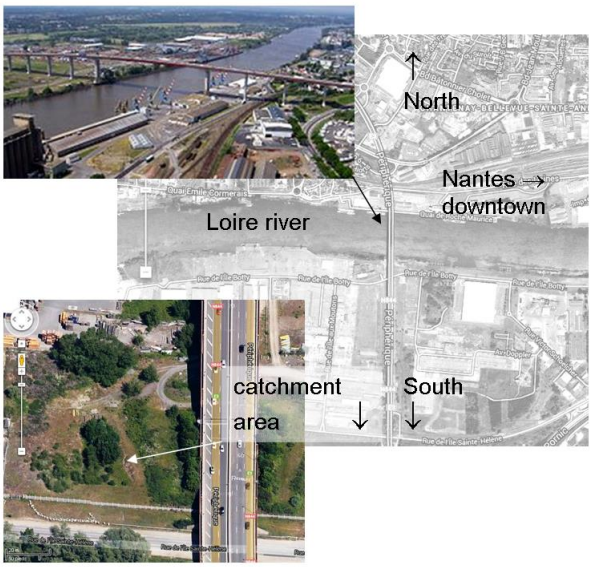

Fig.2 Cheviré bridge (near Nantes) and the catchment area

Catchment area is less representative, in terms of sampling area for the collecting of particles deposited on the road surface, than the road surface under traffic. However, the collecting is easier to carry out as there is no need to close road lanes. On the other hand, particles cannot be collected directly and sediments are first sampled as shown in figure 3a.

a)  b) 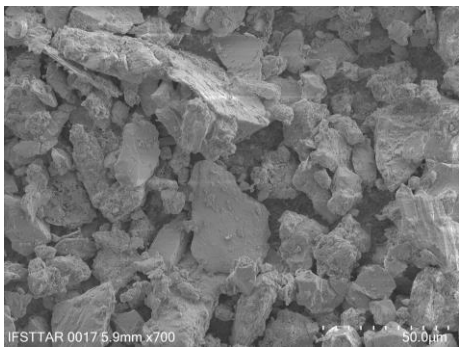

Fig.3 Sample from the catchment area (a: sediments from which particles are extracted; b: particles in their final state of preparation)

The sediments are oven dried in laboratory at 40°C for 4 days. Sieving is then performed to keep only particles smaller than 100 µm. A SEM (Scanning Electron Microscopy) visualization of the particles in their final state (ready for use) is shown in figure 3b. Once can observe that particles exhibit various sizes and shapes.

The choice of fines particles is justified by the fact that coarse fractions are either not fixed on the road surface or crushed by the traffic [25][26] and so only fine particles, which "stick" to the road surface, would have an effect on skid resistance. Four particles' size fractions are extracted: 0-40 µm, 40-50 µm, 80-100 µm and 0-100 µm. The selected particles size fractions are based on previous studies [17] which pointed out that the lubrication mechanisms (sliding, shearing and rolling) induced by a particle layer depend on its thickness and the particle size, which is around 50-60µm.

Particles are analyzed after drying and sieving. Particle size measurement was carried out using low angle laser light scattering with a Malvern Instruments Ltd. A refractive index of 1.53 was used for particles. Results are shown in figure 4.

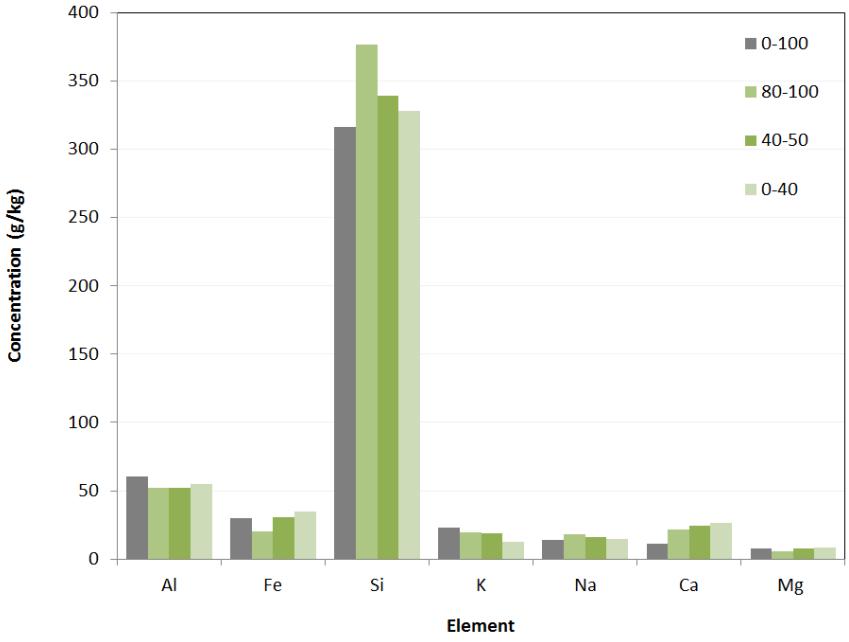

a)

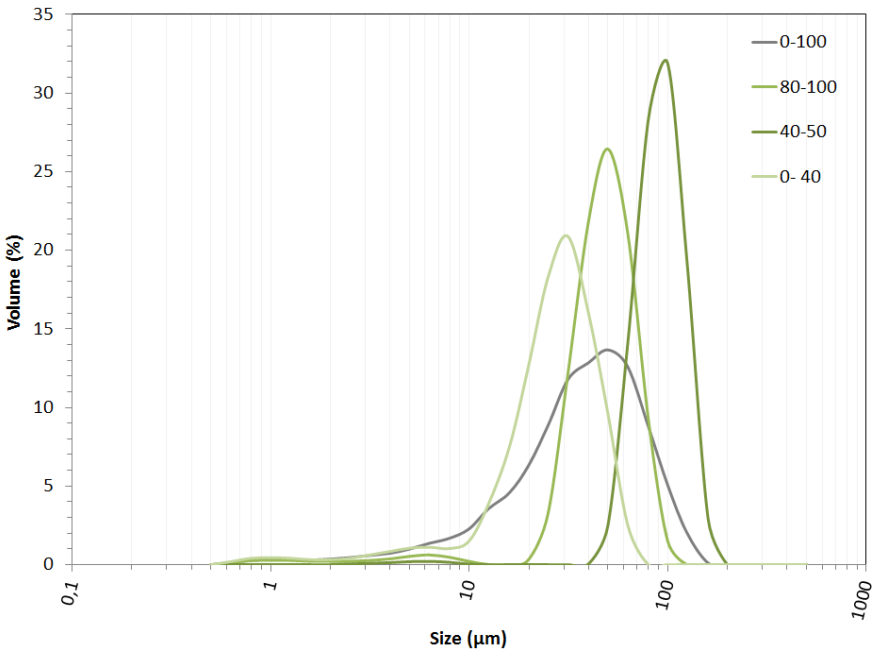

b)

Fig.4 Particles characteristics of the different particle size fractions (a: chemical composition; b: size distribution

As no data is available with respect to the characteristics of particles collected directly on roads, comparisons could be made only with the literature (not very many either). Chemical analysis shows that the particles of the present study are mainly composed of silica which is a hard mineral. The presence of Na, K and Mg can be explained by industrial sites located next to the Cheviré bridge. Some metallic components such as Al, Fe can be attributed to the wear of braking system and tires. In terms of size distribution, comparison is made between fraction 0-100µm and equivalent particles' size from reference [5]. Values at 10%, 50% and 90% are respectively 12.7 µm, 43.8 µm and 92.3 µm. These values are lower in the fine part and higher in the coarse part than those found on particles collected directly from the roads by vacuum (respectively 5.8 µm, 22.3 µm and 112.1 µm) [5]. The range (difference 10% and 90% thresholds) is however inside that of reference [5].

3.3. Particles deposit and compaction

Three quantities of dry particles are used: 0.1g, 0.2g and 0.4g. In terms of concentration (with a surface of 0.01 m^2, see 2.1), they represent respectively 10 g/m^2, 20 g/m^2 and 40 g/m^2. The quantity of 0.2g is first chosen because the surface covered by the particles is similar visually to road surfaces after a long dry period (Fig. 5c); the two other quantities are then chosen as lower and higher limits. References [27] and [28] reported respectively that particle concentrations vary from 20 to 55 g/m^2 and from 10 to 35 g/m^2 for urban streets. In the

absence of data for other types of road networks, it can be said that these number support the relevance of the concentrations selected in this study.

a)

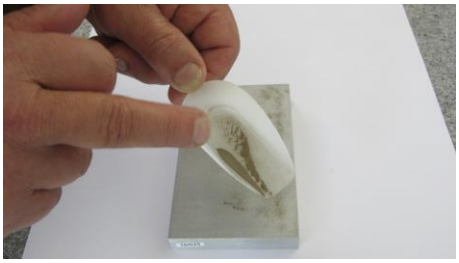

b)

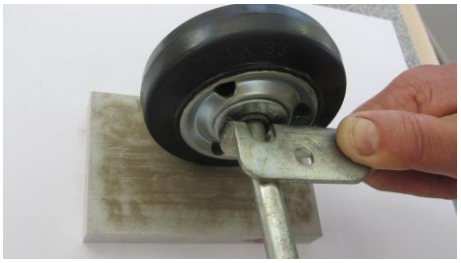

c)

Fig.5 Simulation of particle deposit (a: spreading; b: compaction; c: surface covered by particles)

Spreading of particles on the test surface is done manually (Fig. 5a). The particles are then compacted manually (simulation of vehicular traffic) by means of a small wheel mounted on a metallic arm (Fig. 5b). This method can seem to be rudimentary. Other methods have been tested, for example using a small wheel equipped with a rubber tire and pressed against the surface of the sample by means of screws which make it possible to apply a constant vertical force. However, this method provides a non-homogenous distribution of the particle layer on the surface of the sample. Therefore, while efforts are still developed to look for an operator-independent compaction method, the manual compaction was adopted in this study because it provides the most homogeneous compacted particles' layer. Specimens are subjected to repeated passes (60 passes) of the wheel. Care is taken to apply as much as possible the same wheel pressure to obtain a homogenous distribution of the particles.

3.4. Friction measurement

Friction is measured by means of the so-called Skid Resistance Tester Pendulum (Fig. 6). This device was originally designed by the Road Research Laboratory [29] as an easily-transported static device to make spot-checks on road surfaces, and is widely used throughout the world; a European standard exists to specify the test conditions [30]. It contains, at the end of its articulated arm, a rubber pad that slides on the surface to be measured. The pendulum arm is locked in a horizontal position and the road surface is thoroughly wetted. The arm is then released and allowed to swing freely, being caught by the operator on the backswing after it has reached its maximum height. The maximum height of the pendulum rise is identified by a needle positioned in front of a scale directly graduated to show readings of "friction coefficient measured by the pendulum".

Friction sliders are provided by the Pendulum builder and made of CEN rubber with hardness (IRHD) of 55 (see [31] for specified characteristics). They are wrapped in an opaque envelope and stored in a fridge until the day of testing. Before each test series, the friction slider is subjected to five releases on a surface composed of aggregates. This operation helps to remove the sharp edge of the slider prior to testing the test surfaces.

Fig.6 Skid Resistance Tester Pendulum

3.5. Test procedure

A test series comprises the following steps:

- On the dry and clean surface (step numbered 0): measurement of 3D height cartographies; weighing of the sample (mass m_0); friction measurement.
- Particles are deposited and compacted.

- On the contaminated surfaces (step numbered i, i ≥ 1): weighing of the sample (mass $m_{sample,i}^{before}$); friction measurement on dry-contaminated surface; weighing of the sample after friction measurement (mass $m_{sample,i}^{after}$).
- Steps (i) are repeated until values of the friction coefficient of three successive steps do not differ more than ± 0.01. End of the test series.

The friction slider is wiped after each friction run to remove particles that accumulate at the slider edge. A new rubber slider is used for each test series and it is weighed at the beginning and the end of each test series.

With respect to the end of each test series, we had to define a conventional criterion to stop friction measurements. This criterion is based on the fluctuation of the friction coefficient between successive runs; a tolerance of ± 0.01 between three successive runs was found to be a reasonable criterion.

3D height cartographies are measured on three areas of 5mm × 5mm in dimensions: one at the center and two at the two extreme ends of the specimen (where the friction slider respectively touches and leaves the test surface). A high resolution optical system, based on the focus variation principle [32], is used. Attempts were made to measure cartographies on contaminated surfaces. However, analysis of these cartographies is biased by the fact that artificial roughness is created by humps of particles. The texture analysis of contaminated surfaces, which was thought theoretically as relevant to evaluate the distribution of the particle layer on the test surface at each step, was then not continued.

Weighing is performed by means of a Sartorius Cubis® machine with a reading precision of 0.001g. The sample is cleaned at the end of each test series in a water bath using a Fisherbrand™ ultrasonic cleaner then dried at ambient temperature during at least 2 hours before a new test series.

Due to particle flows, the state of the test surface evolves with friction runs. Inside each test series, the value of friction coefficient recorded at each friction run is then linked exclusively to the corresponding contamination state. However, a complete test series can be repeated to check the consistency of the results. Results in Figure 7 show that values of the friction coefficient at every step are very repeatable (coefficient of variation – ratio standard deviation/mean – less than 4% at each step for the example in Figure 7). These results allow to be confident in the repeatability of the tests.

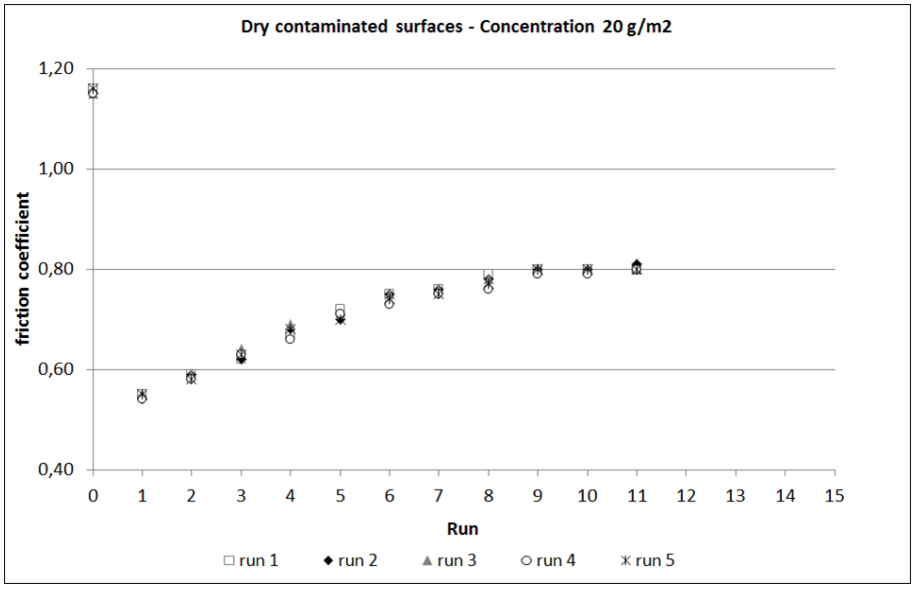

Fig.7 Example of repeated test series (particles' concentration: 20 g/m2; fraction: 0-40µm).

4. Results

4.1. Friction analysis

The friction evolutions of contaminated surfaces for the four particle size fractions with concentrations of respectively 10 g/m^2, 20 g/m^2 and 40 g/m^2 are presented in figure 8. The friction coefficient of contaminated surfaces (steps i; i ≥ 1) is always lower than that of clean surface (step 0). For the three particle concentrations, the evolution of the friction coefficient follows the same tendency: friction coefficient is lowest at the beginning (step 1) then increases progressively with increasing number of slider passes until reaching a stable value. The influence of the particle size fraction is seen for the three concentrations. Friction measured on the coarsest particles (80-100µm) increases rapidly after step 1 and stabilizes at a value close to the friction coefficient of a dry-clean surface expressed as μ_{dry}. The finest fraction (0-40µm) induces a slower increase and a lower stable friction value. It can be seen that the friction variation for the size fraction 0-100µm is similar to that of the finest fraction (0-40µm). This observation might indicate that the friction behavior of the 0-100µm fraction is governed by that of its finest particles.

a)

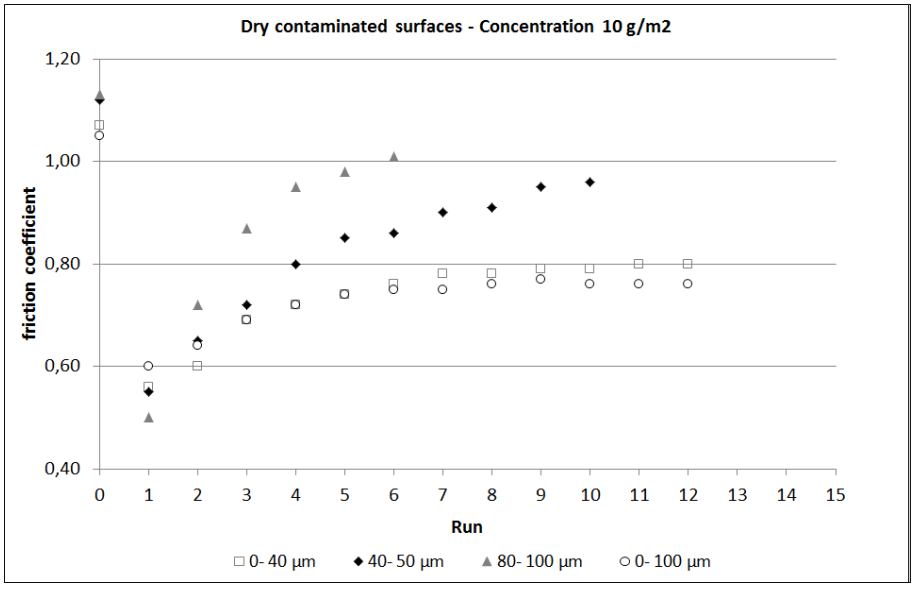
Dry contaminated surfaces - Concentration 10 g/m2
friction coefficient
1,20
1,00
0,80
0,60
0,40
0 1 2 3 4 5 6 7 8 9 10 11 12 13 14 15
Run
0- 40 µm
40- 50 µm
80- 100 µm
0- 100 µm

b)

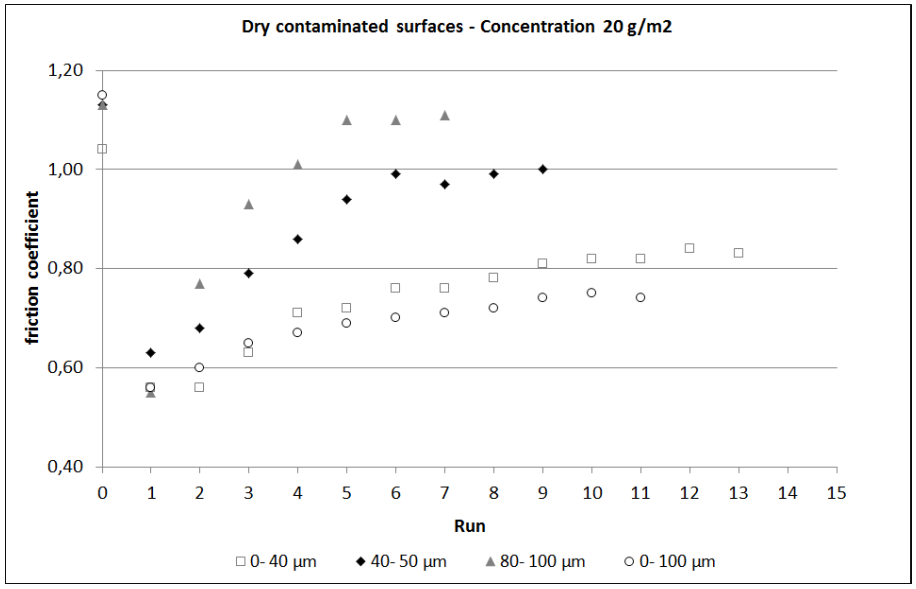
Dry contaminated surfaces - Concentration 20 g/m2
friction coefficient
1,20
1,00
0,80
0,60
0,40
0 1 2 3 4 5 6 7 8 9 10 11 12 13 14 15
Run
0- 40 µm
40- 50 µm
80- 100 µm
0- 100 µm

c)

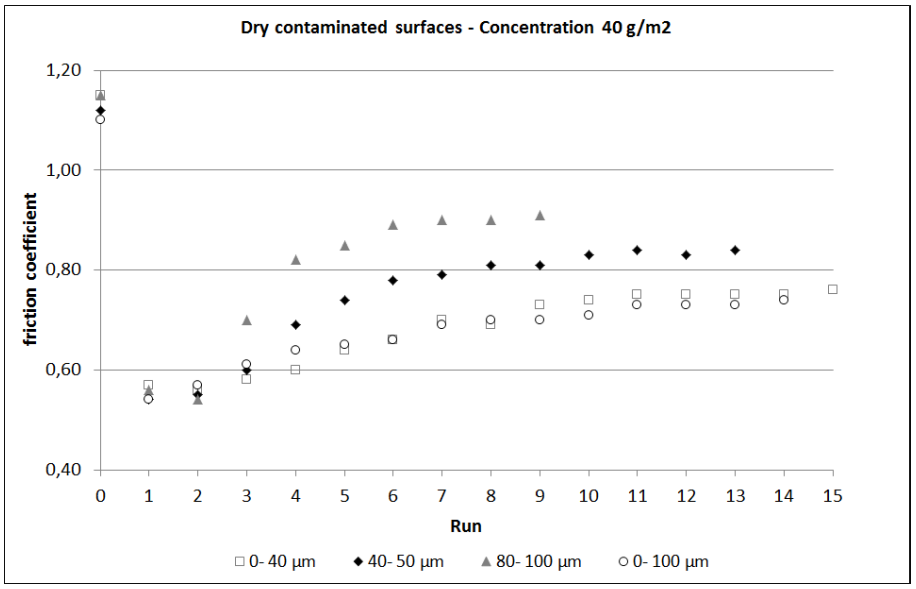
Dry contaminated surfaces - Concentration 40 g/m2
friction coefficient
1,20
1,00
0,80
0,60
0,40
0 1 2 3 4 5 6 7 8 9 10 11 12 13 14 15
Run
0- 40 µm
40- 50 µm
80- 100 µm
0- 100 µm

Fig.8 Variation of friction on contaminated surfaces with particles' size fraction (a: concentration 10 g/m^2; b: concentration 20 g/m^2; c: concentration 40 g/m^2).

SEM observations of the test surface were made at three different steps (clean surface, surface after compaction of the particle layer, and surface after 5 friction runs). It can be seen on the one hand that after compaction particles recover almost completely the sample surface (Fig. 9b) and, on the other hand, that residual particles (Fig. 9c) are less than 40µm in size (Fig. 9d).

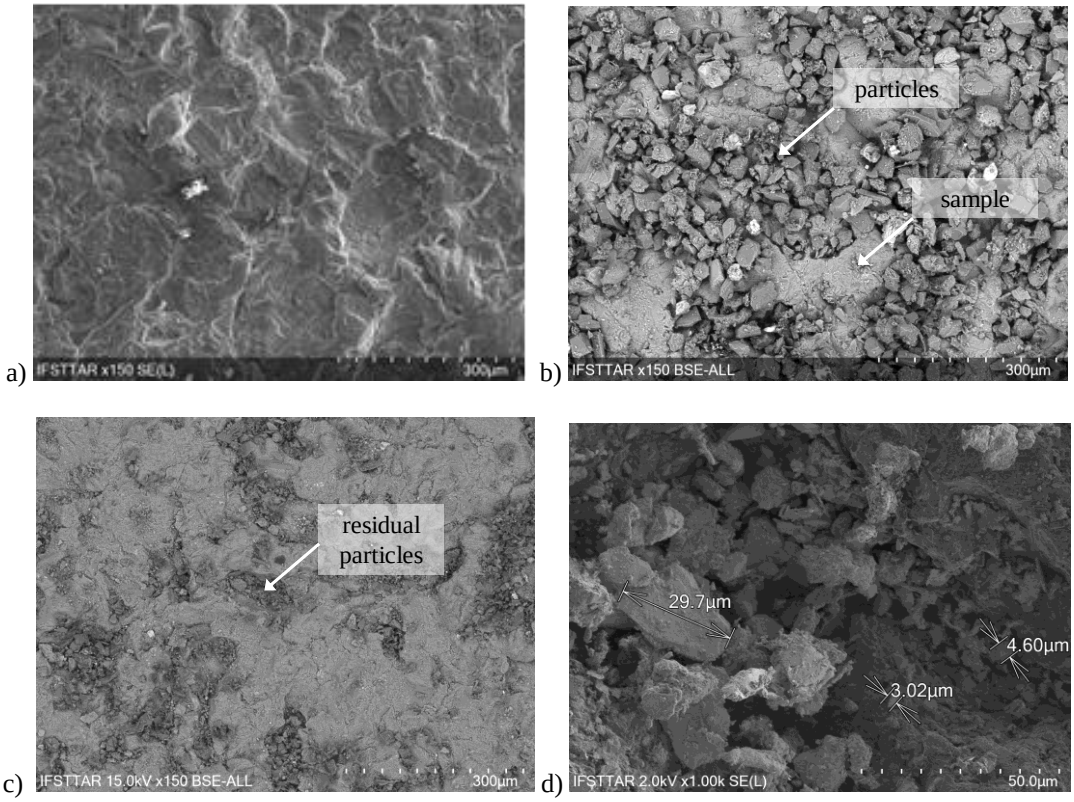

Fig.9 SEM visualizations of the surface of the sample (a: clean surface; b: surface recovered by particles (fraction 0-40µm); c: surface after 5 friction runs; d: close view of residual particles).

Based on SEM photos (Fig. 9b), it is assumed that when friction reaches a minimum at step 1, the test surface is fully covered by a film of particles. Two friction values are then extracted from the friction curves in figure 8: the friction coefficient at step 1, called μ_{lub}, and the mean friction coefficient at the final steps (when the friction coefficient stabilizes), called μ_{stab}, which it is calculated by averaging three final friction measurements. Variations of μ_{lub} and μ_{stab} with the particles' size fraction for different particle concentrations are shown respectively in figures 10a and 10b.

a)

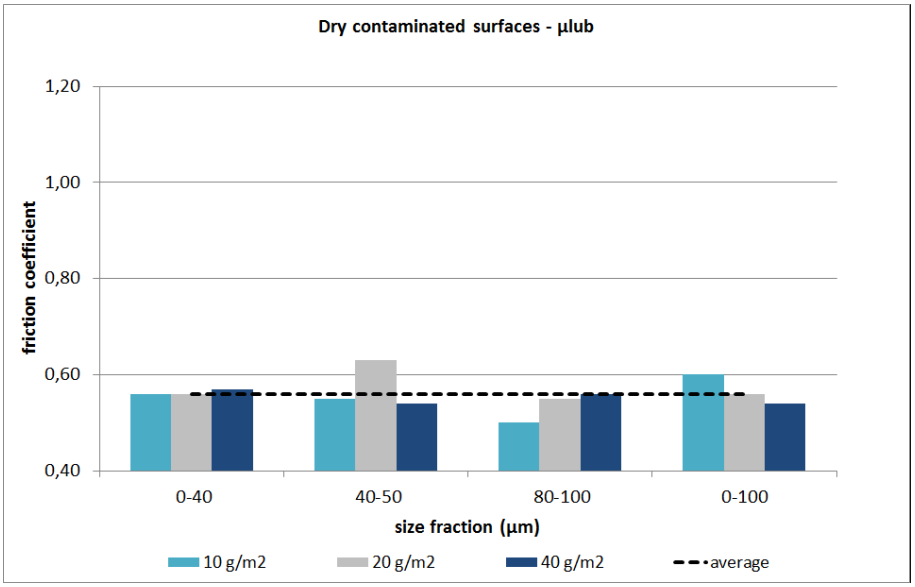

b)

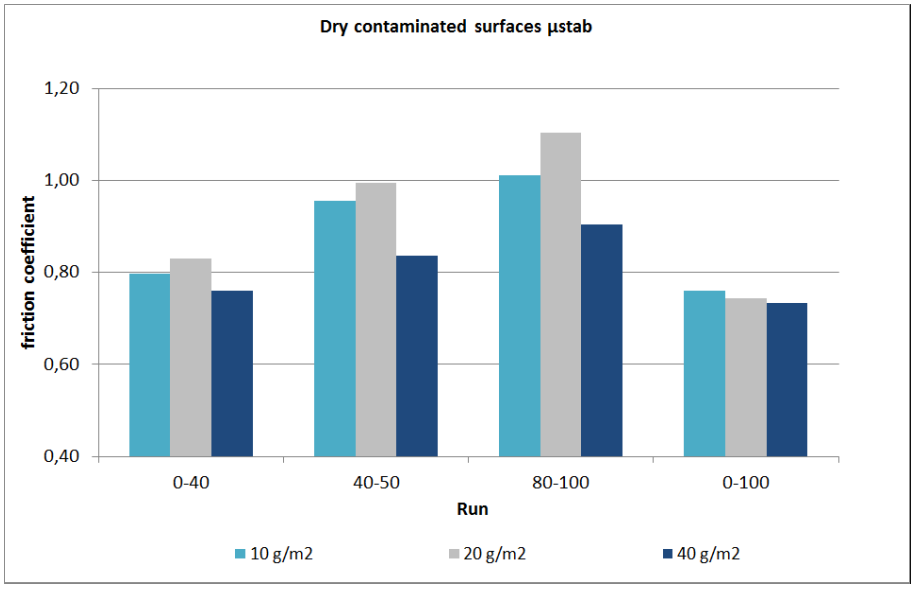

Fig.10 Variations of μ_{lub} (a) and μ_{stab} (b) for different particles' size fractions and concentrations

It can be seen that there is no clear relationship between μ_{lub} and the particles' size fraction and concentration; a grand average (mean value for all fractions and all concentrations) is found to be $\mu_{lub} = 0.56$ (dotted line in Fig. 10a). The dependence of μ_{stab} on the particles' size fraction is more visible. It can be seen from figure 10b that μ_{stab} increases for increasing particle size. The case of fraction 0-100µm is not included in the analysis of the influence of the size fraction because it covers the three other fractions. SEM photos (Fig. 9) confirm visual observation of the test surface after a test series following which the surface is almost clean when it is covered initially by fraction 80-100µm and, conversely, spots of particles are still present when it is covered by fraction 0-40µm. Actually, as the surface's troughs can store only particles smaller than 40µm, the observed spots of particles in fraction 0-40µm correspond to trapped particles. On the other hand, particles in fraction 80-100µm

are too coarse and were probably ejected from the test sample by the friction slider. Values of μ_{stab} depend then on the residual quantity of particles on the surface. The fact that μ_{stab} depends also on the initial concentration reveals another complexity. Actually, μ_{stab} follows a kind of polynomial curve (a form of hump) with the highest friction coefficient at concentration 20 g/m^2. It shows that the initial supply of particles helps increase friction but there is a threshold (between 20 g/m^2 and 40 g/m^2 in the present study) above which friction can drop.

Variation of friction on surfaces contaminated by fine particles (Fig. 8 and the special cases of μ_{lub} and μ_{stab} in Fig. 10) confirms some evidences (contaminated surfaces are more slippery than clean surfaces) but also reveals some complexities when one considers the effect of particles' size and concentration. The initial and residual quantities of particles seem both to govern the friction variation. There is then a need to go further in the analysis to understand what happens at the friction slider/test sample interface. As the quantities of particles seem to be a crucial factor, it was thought that the analysis of mass of particles can be a relevant approach. Actually, as mentioned in section 2 (Research methodology), Fillot et al. [22] have shown that the analysis of the wear-induced particles' mass and its link with particles' flows can help to better understand the movement of particles inside the contact et better interpret wear laws. Given the similarities between Fillot and coauthors' study and our study (movement of dry particles trapped between two rubbing surfaces), we think that the same approach can be adopted for our study to better interpret friction variations.

4.2. Mass analysis

4.2.1 Calculation of particle mass from weighing

Weighing of the rubber slider shows that its mass loss during a test series is negligible (few milligrams) compared with the mass of introduced particles (hundreds of milligrams). Weighing of the sample at the beginning/end of each test series – clean state – shows that its weight does not change. The quantity of detached particles from the two contacting bodies (slider and sample) is then negligible and it was assumed in the following paragraphs that the weight difference between a contaminated sample and the dry-clean sample represents only the mass of the particles.

From weighing (see test procedure), the mass of particles before and after friction tests can be extracted as follows:

$$m_{particles,i}^{before} = m_{sample,i}^{before} - m_0$$
$$m_{particles,i}^{after} = m_{sample,i}^{after} - m_0 \quad (1)$$

where $m^{before}_{particles,i}$ is the mass of particles at step (i) before friction measurement; $m^{after}_{particles,i}$ is the mass of particles at step (i) after friction measurement; $m^{before}_{sample,i}$ is the mass of the sample at step (i) before friction measurement; $m^{after}_{sample,i}$ is the mass of the sample at step (i) after friction measurement; and m_0 is the mass of the clean and dry sample.

4.2.2 Relationship between friction and mass of particles before friction measurement

Figure 11 shows the friction variation with particles' masses before (Fig. 11a) and after (Fig. 11b) friction measurements. It can be seen that trends are very similar. This result can be explained by the fact that the mass of particles after friction measurement at step (i) is the one before friction measurement at step (i+1), i.e., $m^{after}_{particles,i} = m^{before}_{particles,i+1}$; the graph in figure 11b is just a translation to the left of the one in figure 11a (with data at step 1 in less). In the following sections, analysis of the relationship between friction and particles mass is then made only for the mass before friction measurement.

It can be seen that the friction and particles' mass variations are identical but in the opposite directions: less particles induce more friction. Mills et al. [17] explained that there is a shear effect when the slider sweeps the particle layer and the initial layer of particles thins (and so the particles' mass decreases) to the point where the slider-surface asperity contact is restored. This mechanism can explain why friction starts from a minimum value (shearing mechanism), then increases with successive passes of the slider (sliding mechanism with partial contact between the rubber slider and the surface asperities).

a)

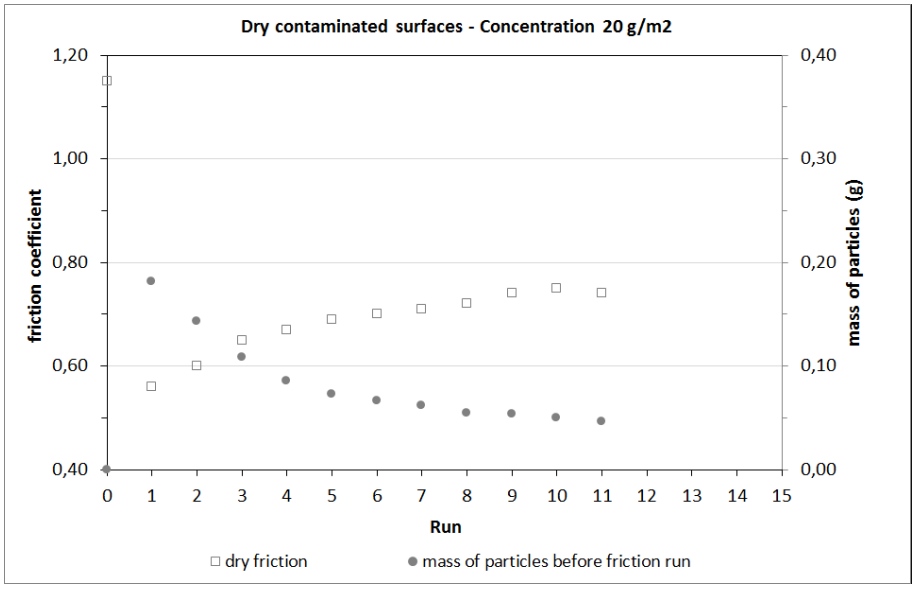

b)

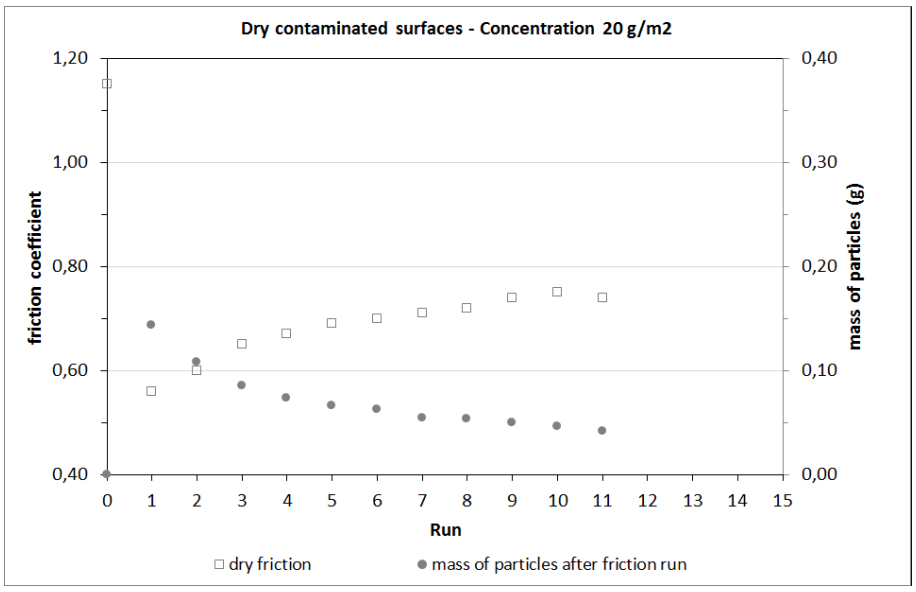

Fig.11 Variation of friction coefficient and particles mass (a: mass before friction measurement; b: mass after friction measurement)

Figure 12 shows the relationship between friction and mass of particles for the four particles' size fractions at concentration 40 g/m^2 (the same trend is observed for the two other concentrations). In addition to the fact that less particles induce more friction, two other observations can be made. The first one is that there is a sharp increase of friction at the left end of the graph (particles' mass lower than 0.05g). This observation was also made by Heshmat [18] for powder layers and this author attributes the sharp increase of friction to the breaking of the particle layer and then the beginning of direct contact between the two contacting bodies (considering powder as a third body).

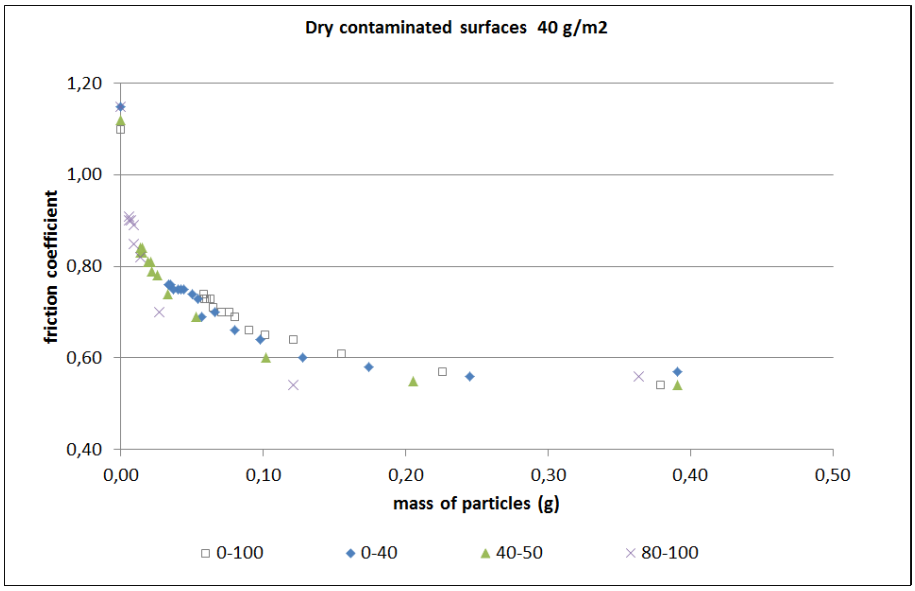

Fig.12 Variation of friction coefficient with particles mass (all particles' size fractions at a given concentration)

The second observation from figure 12 is that all particles' size fractions, despite their very different behaviors (Fig. 8c, which corresponds to the example shown in figure 10), follow the same trend. To confirm this observation, the graph in figure 12 was reproduced with data from all fractions and all concentrations. Figure 13 shows actually a tight relationship between friction and particles' mass. Some scatters can be observed compared with figure 12.

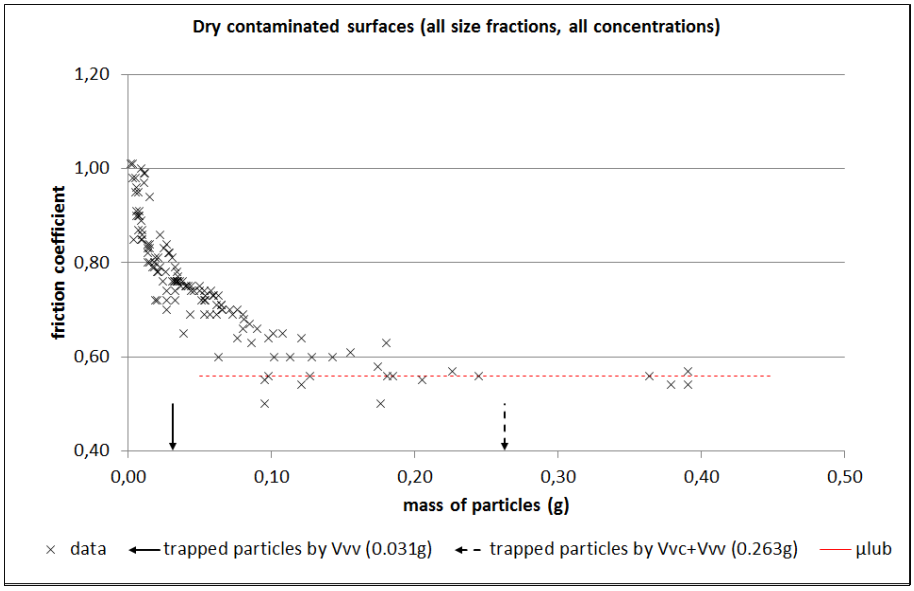

Fig.13 Master curve expressing the variation of friction coefficient with particles mass

4.2.3 Particle trapping

Mills et al. [17] mentioned that when the sample surface is rough, it can induce some particle trapping (illustrated in Figure 14). The presence of trapped particles can explain why the friction coefficient at the end of a test series is lower than that of a clean surface. On the other hand, Fillot et al. [22] have shown in their model of third body flows that if the total mass of particles is higher than the mass of trapped particles (inducing the part surrounded by the dotted line in Figure 14), third bodies – particles – will be ejected from the contact; conversely, if the total mass of particles is lower than the mass of trapped particles, no particle ejection occurs.

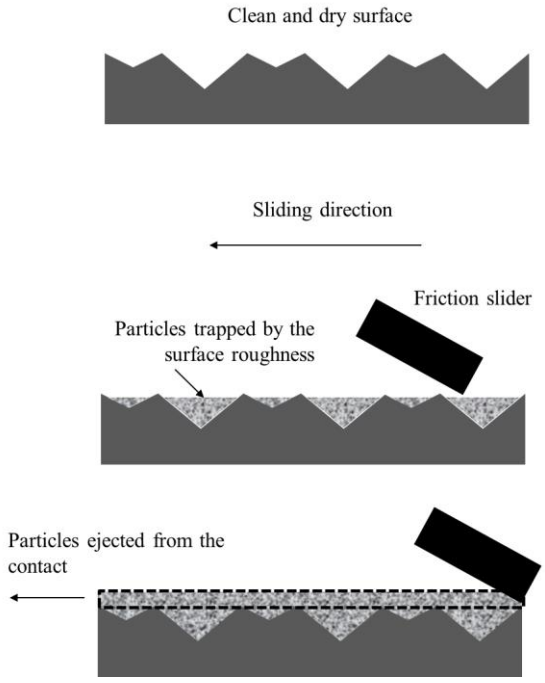

Fig.14 Illustration of the particle-trapping mechanism

Particle trapping is then a mechanism that must be investigated to better estimate particle flows. Attempt is made in this section to estimate the mass of trapped particles for different particles' size fractions and concentrations. Two approaches are envisaged: 1- estimation of the trapped particles by looking at the particle mass at the end of each test series; and 2- estimation of the trapped particles by looking at the available space of the test sample.

The mass of particles measured at the end of test series is shown in figure 15. Each bar represents the average of $m_{particles,i}^{after}$ (mass of particles after friction measurements) of the last three steps (in the test protocol, tests are stopped when values of the friction coefficient of three successive steps do not differ more than ± 0.01).

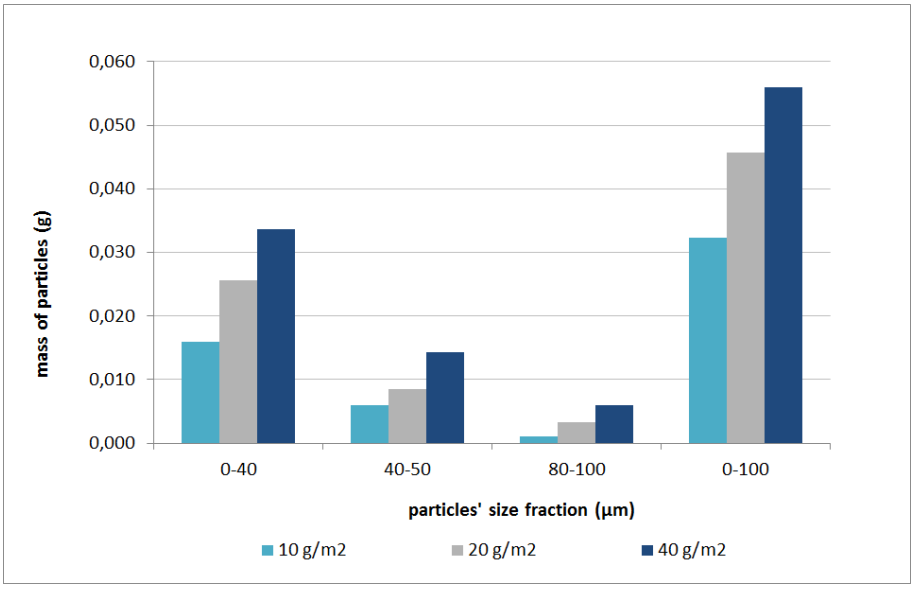

Fig.15 Mass of particles at the end of friction tests

It can be seen that the quantity of trapped particles depends on the particle's concentration and size fraction. For a given size fraction, higher initial concentration induces higher trapped particles. This result, which can seem to be obvious at a first glance, reveals the fact that a stabilization of friction values does not mean a saturation of the surface troughs (where particles are trapped); otherwise, the quantity of particles would be constant regardless of the initial concentration. A stabilization of friction values would then merely mean that particles are no more ejected by the contact between the friction slider and the test surface.

Looking at size fractions of 0-40µm, 40-50µm and 80-100m, it can be seen that finer fractions induce higher quantity of trapped particles. This observation provides an explanation of the friction recovery observed in figure 10b (μ_{stab}). Friction is rapidly recovered for coarse fractions and reaches a value close to that of a clean and dry surface because there is (almost) no more particles present on the surface. Conversely, fine particles accumulate on the test surface and continue to lubricate the slider/test surface interface; friction stabilizes then at a value lower than that of a clean and dry surface.

The fact that there are more trapped particles for the fraction 0-100µm would reveal another feature about the trapping mechanisms. Actually, trapping does not mean simply a filling of the surface troughs. There would be a mechanical interlocking which prevents particles to roll one on the other. The mechanical interlocking is facilitated for fine particles (under 50-60µm after [17]), which are densely packed, and probably for wide particle size's distributions (such as fraction 0-100µm) where the small particles can occupy the interspace between the larger particles [33] and induce finally a dense particle arrangement as well.

For the second approach (estimation of the trapped particles by looking at the available space of the test sample), attempt is made to estimate the quantity of trapped particles from the surface texture considering two volume parameters: sum of $V_{vv} + V_{vc}$ and V_{vv}. The first parameter considers all the troughs of a surface and the second assumes that particles are trapped only in the deepest valleys. From table 2, the available volumes are respectively 175 mm^3 (sum $V_{vv} + V_{vc}$ multiplied by the total surface = 17.52 × 0.01, then converted from ml to mm^3) and 18.2 mm^3 (V_{vv} × total surface). Assuming that fine particles are similar to clay (density of 1700 kg/m^3 or 1.7 10^{-3} g/mm^3), the mass of particles that can be stored is respectively 0.263g (considering $V_{vv} + V_{vc}$) and 0.031g (considering V_{vv}). Values of particles' mass in figure 15 show that particles are mainly trapped in the deepest valleys of the test surface. Less trapped particles for fractions 40-50µm and 80-100µm would mean that these particles are too coarse with respect to the dimensions of the deepest valleys and only part of them can be stored.

The two values 0.031g and 0.263g are injected in figure 13 and provide another insight into the relationship between friction and particles mass. When the particles' mass is lower than 0.263g, it can be said that the friction coefficient starts to increase from a level which corresponds to μ_{lub} (dotted horizontal line at $\mu = 0.56$). If the particles' mass continues to decrease and becomes lower than 0.031g, the increase of friction coefficient is more rapid. One can say that 0.263g represents the theoretical minimum quantity of particles to cover completely all surface asperities. When particles are ejected and the particles' mass is lower than this threshold, some direct contacts are established between the slider and the surface asperities; the friction coefficient becomes then higher than μ_{lub}. Successive runs will eject other particles from the slider/sample contact area. When there are only particles left in the deepest valleys (mass < 0.031g), one can consider that, with respect to lubrication mechanisms, full direct contact is recovered between the slider and the surface asperities.

The reader can raise some contradictions with respect to observations made in figure 10a. Actually, it can be seen in this figure that the friction coefficient μ_{lub} is attained even for particles' mass lower than 0.263g (concentrations of 10 g/m^2 and 20 g/m^2) whereas the sample surface should not be completely covered by a particle layer. Referring to the dry lubrication mechanisms investigated in [17], it can be said that μ_{lub} can be induced by either a sliding/shearing mechanism on a surface completely covered or a sliding/shearing mechanism plus some rolling (induced by free particles) on a surface partially covered. The free particles can cover the surface's asperity peaks (by the deposit process or the sweeping of the slider) and there can be momentarily a full particle layer on a surface partially covered initially. This is just a tentative explanation and the raised point deserves a deeper investigation in the future.

5. Modeling

5.1. Model formulation

From figure 8, it can be said that friction of surfaces contaminated by dry particles is between two extreme values: μ_{dry} (clean surface) and μ_{lub} (surface fully covered, with some reserves as discussed at the end of the previous section). It was seen that the mass of particles, or more exactly, the way by which the test surface is covered by particles, governs the friction coefficient. The friction coefficient of a contaminated surface can be then expressed as:

$$\mu = X.\mu_{lub} + (1 - X).\mu_{dry} \quad (2)$$

where X is the fraction of the surface covered by the particles.

It can be seen that when X = 1 (surface fully covered), $\mu = \mu_{lub}$; when X = 0 (clean surface), $\mu = \mu_{dry}$. The term μ_{dry} expresses the unlubricated friction between the rubber and the test surface and includes preponderant mechanisms like hysteresis (dissipated energy) and adhesion (molecular bonds) [34]. Modeling this term is a very complex task and is beyond the objective of this study. That is why μ_{dry} will be obtained by experiments. From very extensive experiments to study the friction of rubber against hard surfaces, Grosch [34] has also shown that fine powder (magnesia MgO) suppresses the adhesion component of friction even on rough surfaces (silicon carbide paper with particles of 100µm in size). The term μ_{lub} can then include some rubber's deformation losses and mechanisms specific to particulate layers like shearing or rolling as Mills and coauthors highlighted in [17]. The modeling of this term is again beyond the objective of this study and μ_{lub} will be obtained by experiments as well.

Equation (2) is widely used in the literature and there are different ways to express X. Our approach was first based on works published by Higgs et al. [19]. These authors studied the lubrication between a rough surface and a slider by MoS_2 (molybdenum disulfide) particles (sizes varying from 1.56µm to 13.64µm). Fraction X, called fractional coverage in [19], is dimensionless and is defined as:

$$X = \frac{h}{h_{max}} \quad (3)$$

where h is the local height of the third body film; and h_{max} is the maximum value of h (surface fully covered by the particles).

Parameter X was first derived from 3D cartographies measured on contaminated surfaces using, for (h),

respectively parameters S_q, V_{vv} and (V_{vc} + V_{vv}) (see Tab. 2). Values of h_{max} correspond then to values of these roughness parameters at the clean state (step 0). It was found that values of (h) at step 1, and even at further steps, are higher than h_{max}. This surprising result can be explained by the formation of clumps of particles on the top of the surface asperities (as already observed in [35]) which increases artificially the surface roughness. Another way was then sought for the definition of fraction X using the mass of particles.

5.2. Use of the index of starvation

In his experiments and subsequently developed theory of powder lubrication, Heshmat [18] noticed that "… the change in the friction coefficient value is due to the onset and growth of powder depletion with the duration of testing …". This author used a so-called index of starvation which expresses the evolution of the powder film from a full-film state to a partially-broken state and defined it as the ration of available powder to the powder for full film. In the present study, using the mass of particles, an index of starvation is calculated the available quantity of particles at each step, i.e., $m^{before}_{particles,i}$, divided by the initial quantity of particles after compaction, i.e., $m^{before}_{particles,1}$:

$$\text{Index of starvation at step (i)} = I_{starv,i} = \frac{m^{before}_{particles,i}}{m^{before}_{particles,1}} \quad (4)$$

The index of starvation I_{starv} has the same meaning as the fractional coverage X because the mass of particles $m^{before}_{particles,i}$ corresponds somewhat to the local height of third body film h; and $m^{before}_{particles,1}$ is the maximum of $m^{before}_{particles,i}$. Moreover, I_{starv} is relevant for the present study which has highlighted the role of the mass of particles in the friction phenomenon. We can finally check that for I_{starv} = 0 (no particle) $\mu = \mu_{dry}$ and for I_{starv} = 1 (surface fully covered) $\mu = \mu_{lub}$.

First attempts using equation (2) with X = I have shown that the model does not always fit the experiments. Example in figure 16 shows that the model overestimates friction values.

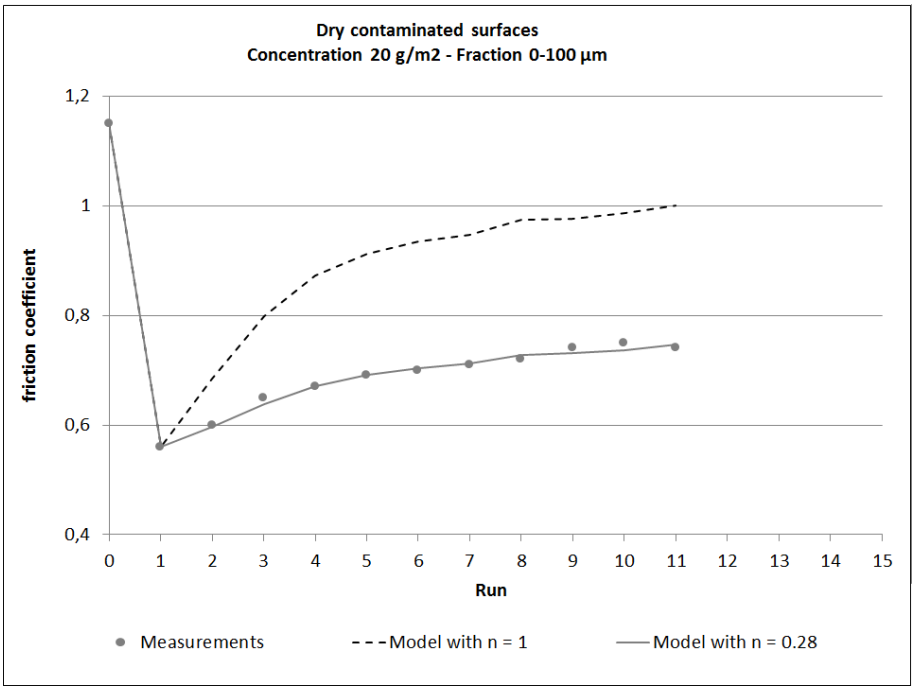

Fig.16 Quality of model fitting using X = I_{starv}^{n} with n = 1 and n = 0.28.

It was found that adding an exponent (n) to I_{starv} gives better results (n = 0.28 for the example shown in Fig. 16). The final form of the model tested in the present study is:

$$\mu = I_{starv}^{n}.\mu_{lub} + (1 - I_{starv}^{n}).\mu_{dry} \quad (5)$$

where I_{starv} is the index of starvation; μ_{dry} and μ_{lub} are obtained from friction measurements at respectively step 0 and step 1; and n is an exponent to be determined.

5.3. Results

Figure 17 shows the comparison between the model and the experiments. It can be seen that the proposed model reproduces very well experimental results, in particular the increase of friction coefficient from the minimum and its stabilization. The lines representing the model is not smooth because the particles' mass (and so the index of starvation) does not evolve smoothly between successive steps. The relative error between the model and experimental values is less than 2% for all particles' sizes and concentration; it confirms the accuracy of the model.

a)

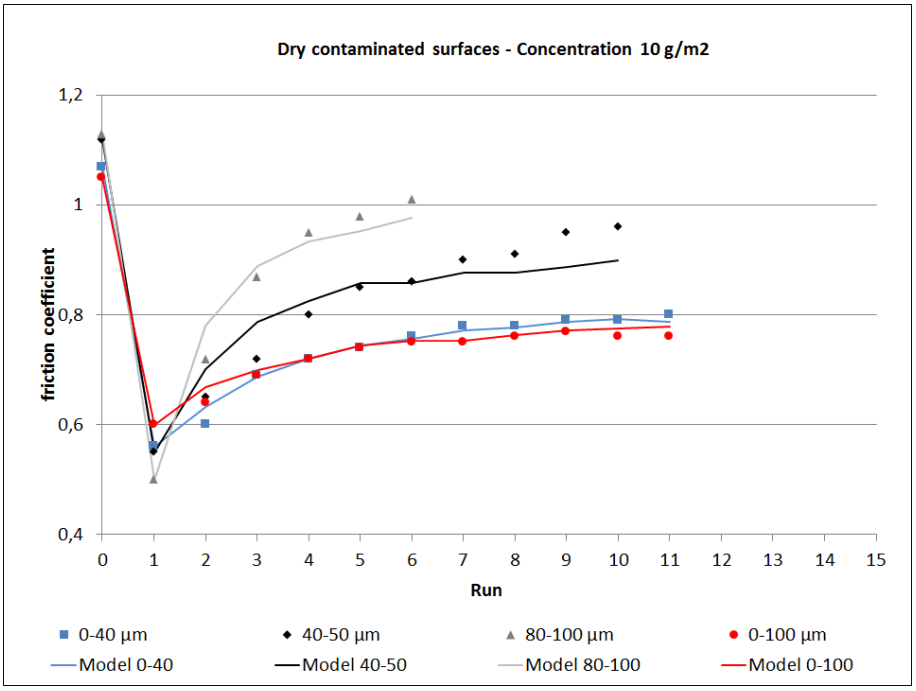
Dry contaminated surfaces - Concentration 10 g/m2
friction coefficient
Run
0-40 µm
40-50 µm
80-100 µm
0-100 µm
Model 0-40
Model 40-50
Model 80-100
Model 0-100

b)

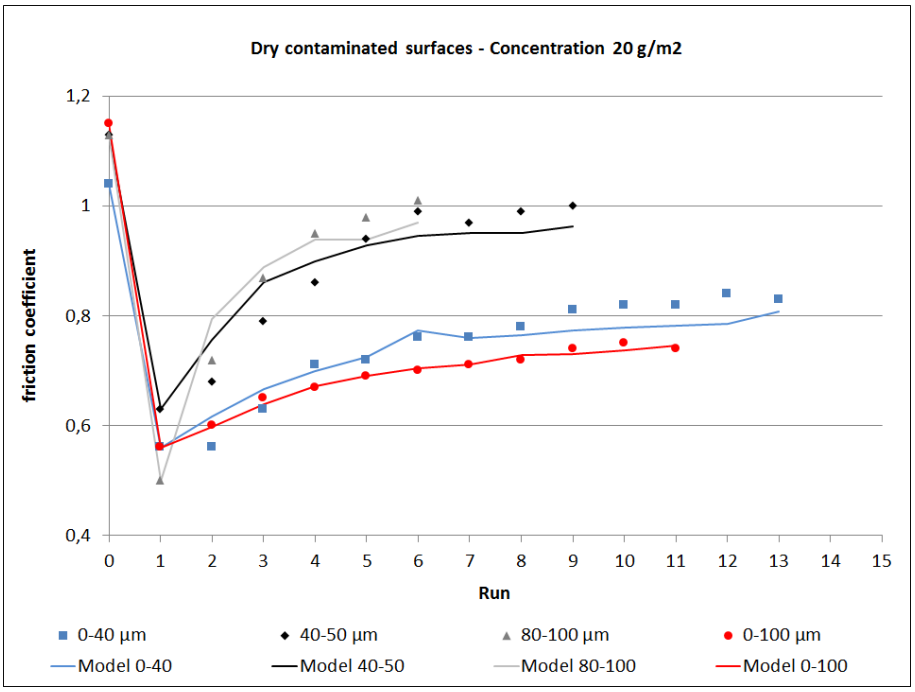
Dry contaminated surfaces - Concentration 20 g/m2
friction coefficient
Run
0-40 µm
40-50 µm
80-100 µm
0-100 µm
Model 0-40
Model 40-50
Model 80-100
Model 0-100

c)

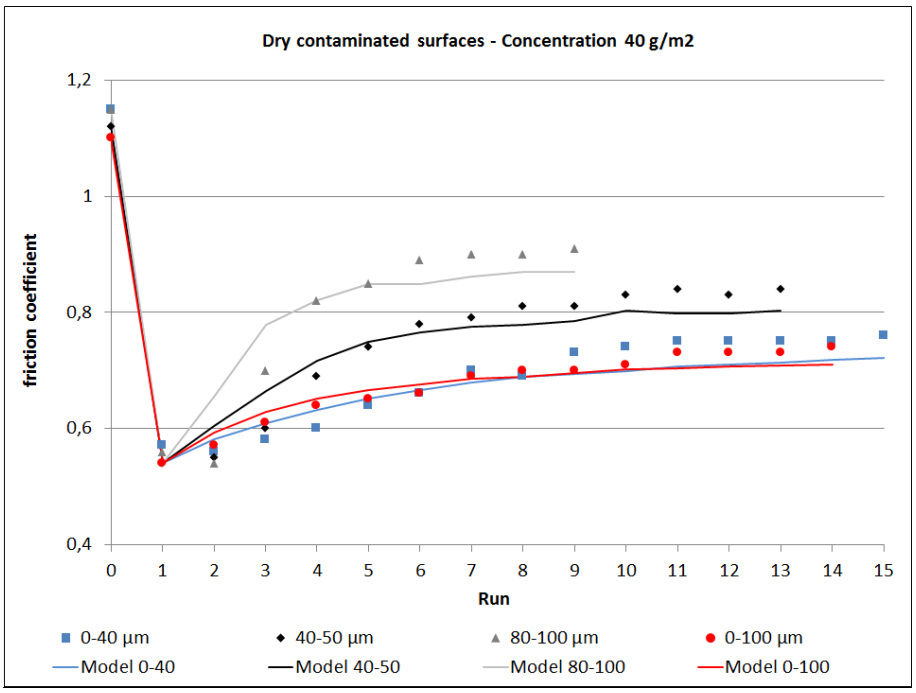

Fig.17 Model versus experimental results for all particles' size fractions and concentrations

Values of exponent (n) are summarized in table 3. Values of (n) globally decrease when the particles' concentration increases and does not depend on the particles' size fractions for a given concentration. For the three studied concentrations, (n) takes respectively the values of 0.37, 0.33 and 0.18.

Tab.3 Values of exponent (n)

Fraction (µm)	**Concentration**		
	10 g/m^2	**20 g/m^2**	**40 g/m^2**
0-40	0.35	0.33	0.16
40-50	0.34	0.37	0.18
80-100	0.37	0.34	0.19
0-100	0.41	0.28	0.19
Average all fractions	0.37	0.33	0.18

To understand the meaning of exponent (n), graphs representing the variation of the friction coefficient with the index of starvation were plotted for different particles' size fractions and concentrations (Fig. 18). For each particle concentration, the index of starvation is raised to the corresponding power (n) (average values in Tab. 3).

a)

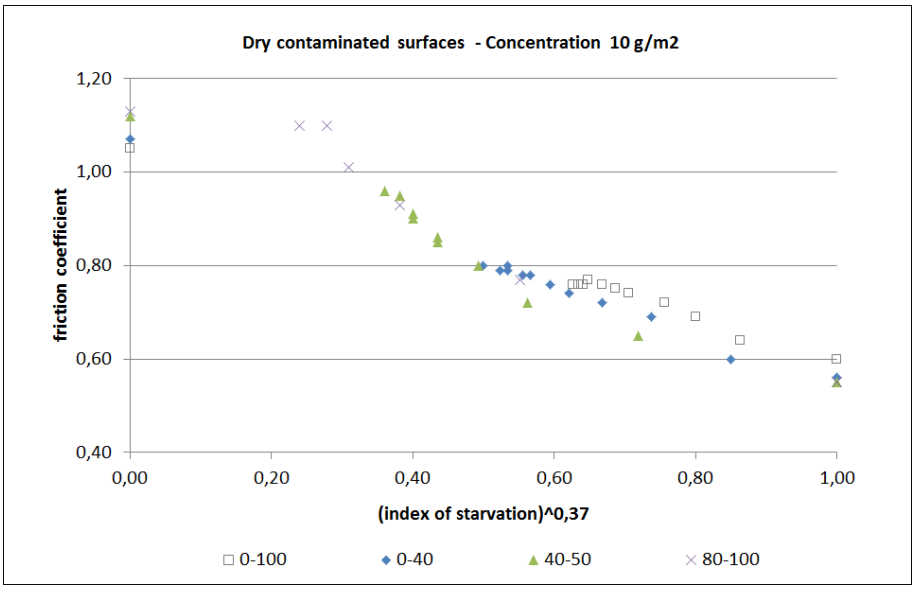
Dry contaminated surfaces - Concentration 10 g/m2
friction coefficient
1,20
1,00
0,80
0,60
0,40
0,00
0,20
0,40
0,60
0,80
1,00
(index of starvation)^0,37
0-100
0-40
40-50
80-100

b)

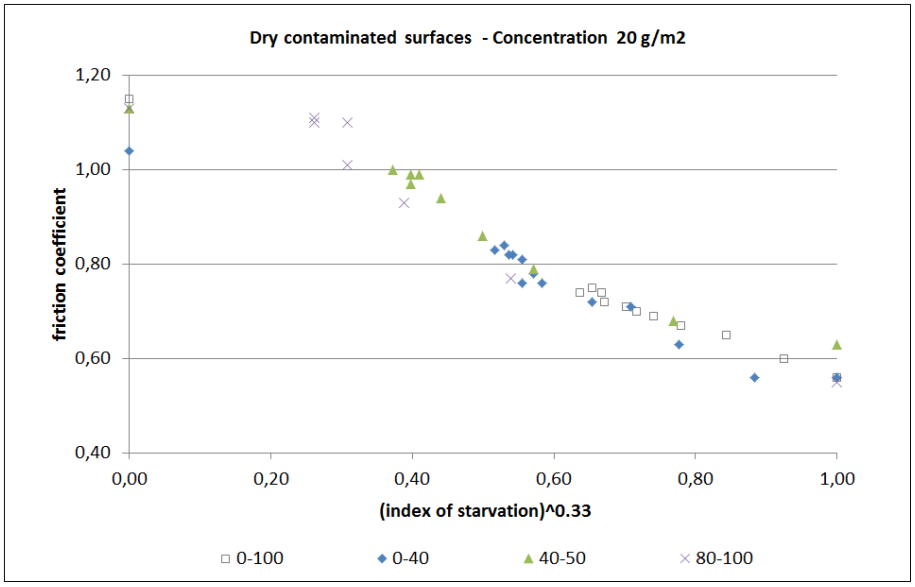
Dry contaminated surfaces - Concentration 20 g/m2
friction coefficient
1,20
1,00
0,80
0,60
0,40
0,00
0,20
0,40
0,60
0,80
1,00
(index of starvation)^0.33
0-100
0-40
40-50
80-100

c)

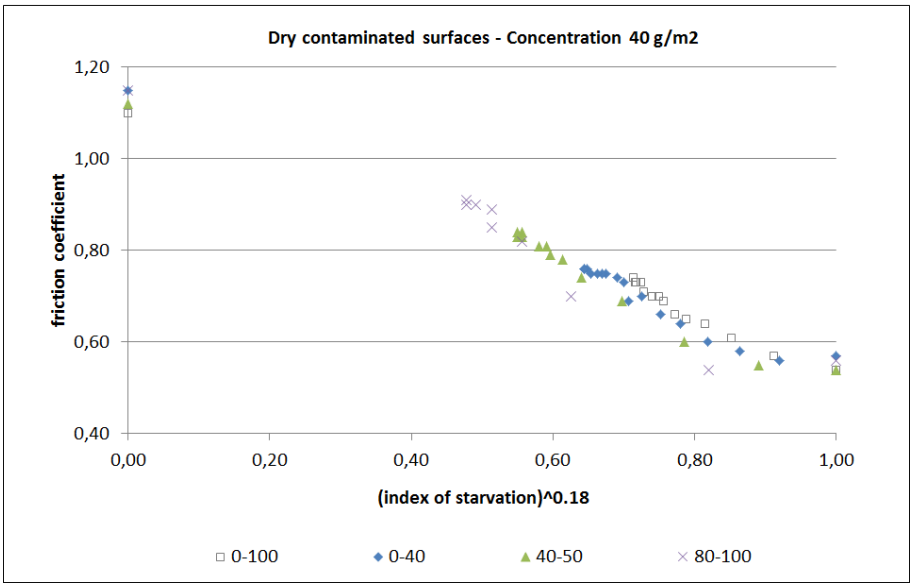

Fig.18 Variation of friction evolution with the index of starvation.

It can be seen that, for each concentration, the friction-index of starvation plots follow a master curve which is similar to the Stribeck curve widely used in fluid-lubricated contacts (Fig. 19). Compared with the curve in figure 19, the graphs in figure 18 do not show any increase of friction coefficient in the hydrodynamic regime.

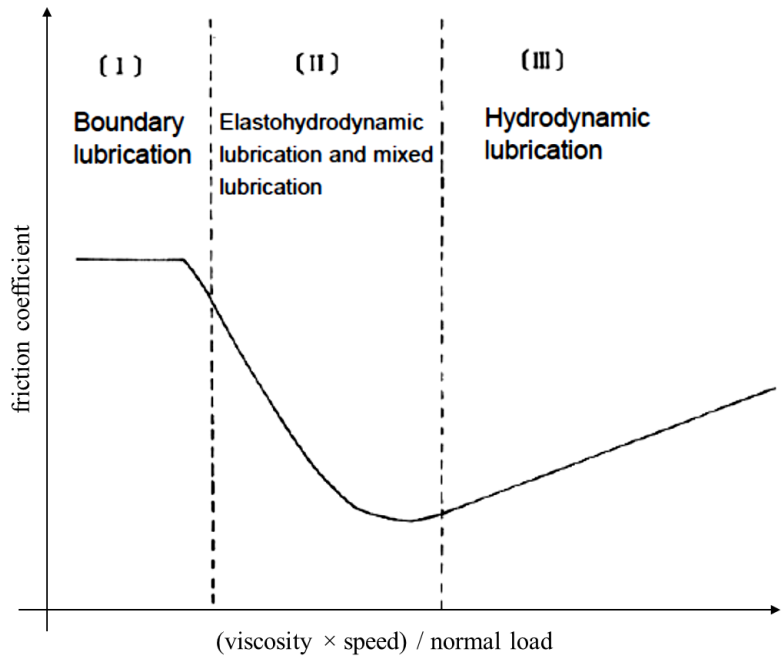

Fig.19 Example of Stribeck curve.

Our observation corroborates that of Heshmat for powders [18]. This author observed a sudden rise of the

friction coefficient at an index of starvation of 20%. In the present study, we observe rather a progressive increase (starting from a fully covered surface at the right side of the graphs) of the friction coefficient before reaching (see mainly the graphs for 20 g/m^2 in concentration) a plateau. We cannot confirm at this moment that the three phases (that are mainly visible in figure 18b) correspond respectively to the boundary, mixed and hydrodynamic lubrication regimes. Further tests and analyses would help to clarify this point.

6. Conclusions

In this paper, laboratory tests are conducted to investigate the friction on dry road contaminated by fine particles deposited on the road surface. Particles are collected from a catchment area and sieved to obtain different size fractions. The test protocol simulates the particles' deposit and their compaction by the traffic. Sliding friction tests are conducted to evaluate the evolution of friction coefficient over time as a function of particles' size fraction and concentration.

It was found that friction on contaminated surfaces is lower than friction on a clean surface expressed as μ_{dry}. The friction coefficient is lowest, expressed as μ_{lub}, when the surface is fully covered by a particle layer. Successive runs induce an increase of the friction coefficient to a stable value which can be close to μ_{dry} or well below it. It was found that the friction recovery, and more generally the friction variation, is governed by the mass of particles present on the surface of the test sample.

Weighing of the test sample helps to extract particles' mass. Analyses show that there is a tight relationship between friction and particles' mass: less particles induce higher friction. Explanations are given in terms of thinning of the particle layer by successive passes of the friction slider until asperity contact occurs. Estimation of the quantity of particles trapped by the surface texture helps to better understand the friction-particles' mass relationship. Two mass thresholds were identified from the volume parameters (Abbott's curve). They determine respectively the moment when the friction coefficient increases from μ_{lub} and when it increases sharply to reach μ_{dry}.

A model was proposed to represent the friction coefficient of a contaminated surface as a function of μ_{lub} and μ_{dry} weighted by a function characterizing the surface fraction X covered by particles. It was found that X is best represented by the so-called index of starvation I_{starv} developed for powder lubrication. Rising I_{starv} to an exponent (n) provides very good adjustment of the model to the experiments. Further tests are needed to define the physical meaning of (n).

7. Acknowledgment

The authors thank Patrick Maisonneuve, Christophe Ropert and Jean-François for the realization of all experiments. We also thank Professor Hassan Zahouani for helpful discussions, mainly for having raised the importance of studying the dry lubrication by fine particles.

8. References

[1] D. Eisenberg, The mixed effects of precipitation on traffic crashes. Accident Analysis and Prevention, 36, 637–647, 2004.

[2] J.D.Sartor, G.B. Boyd, F.J. Agardy, Water pollution aspects of street surface contaminants. Water Pollution Control Federation, 46(3), 458-467, 1974.

[3] P. Egodawatta, Translation of small plot scale pollutant build-up and wash-off measurements to urban catchment scale. PhD thesis, Faculty of Built Environment and Engineering, Queensland University of Technology, Australia, 2007.

[4] R.B. Shakely, J.J. Henry, R.J. Heinsohn, Effects of pavement contaminants on skid resistance. Transportation Research Record, 788, 23-28, 1980.

[5] D. J. Wilson, An analysis of the seasonal and short-term variation of road pavement skid resistance. PhD Thesis, University of Auckland, NZ, 2006.

[6] M.T. Do, V. Cerezo, and H. Zahouani, Laboratory test to evaluate the effect of contaminants on road skid resistance. Engineering Tribology, 268 (11), 1276-1284, 2014.

[7] B.T Kulakowski. and D.W. Harwood, Effect of water-film thickness on tire-pavement friction. Surface Characteristics of Roadways: International Research and Technologies, ASTM STP 1031 (W.E. Meyer and J.Reichter, Eds.), American Society for Testing and Materials, Philadelphia, 50-60, 1990.

[8] M.T. Do, V. Cerezo, Y. Beautru, and M. Kane, Modeling of the connection road surface microtexture/water depth/friction. Wear, 302, 1426-1435, 2013.

[9] B.E. Sabey, Pressure distributions beneath spherical and conical shapes pressed into a rubber plane, and their bearing on coefficients of friction under wet conditions, Proc. Phys. Soc., 71, 979-988, 1958.

[10] A.R. Savkoor, Tribology of tyre traction on dry and wet roads, Proceedings of the 17th Leeds – Lyon Symposium on Tribology, pp. 213-228, 1990.

[11] R.F. Lambourn and E. Viner, Friction tests on contaminated road surfaces, Published Project Report PPR073, TRL Ed. Limited, 33 pages, 2006.

[12] B. N. J. Persson, U. Tartaglino, O. Albohr, and E. Tosatti, Rubber friction on wet and dry road surfaces: the sealing effect. Physical Review, B71, DOI: 10.1103/PhysRevB.71.035428, 2005.

[13] Y. Peng, Y. Xu, J. Geng, K.D. Dearn, and X. Hu, Tribological assessment of coated piston ring-cylinder liner contacts under bio-oil lubricated conditions. Tribology International, 107, 283-293, 2017.

[14] X. Zheng, Y. Xu, J. Geng, Y. Peng, D. Olson, and X. Hu, Tribological behavior of Fe3O4/MoS2 nanocomposites additives in aqueous and oil phase media. Tribology International, 102, 79-87, 2016.

[15] Y. Xu, J. Geng, X. Zheng, K.D. Dearn, X. Hu, Friction-induced transformation from graphite dispersed in esterified bio-oil to graphene. Tribology Letters, 63:18, 2016.

[16] K.W. Li, F. Meng, W. Zhang, Friction between footwear and floor covered with solid particles under dry and wet conditions. International Journal of Occupational Safety and Ergonomics (JOSE), 20 (1), 43–53, 2014.

[17] R. Mills, R.S. Dwyer-Joyce, M. Loo-Morrey, The mechanisms of pedestrian slip on flooring contaminated with solid particles. Tribology International, 42, 403-412, 2009.

[18] H. Heshmat, Wear reduction systems for coal-fueled diesel engines – Experimental results and hydrodynamic model of powder lubrication. Wear, 162-164, 518-528, 1993.

[19] C.F. Higgs, E.Y.A. Wornyoh, An in situ mechanism for self-replenishing powder transfer films: Experiments and modeling. Wear, 264, 131-138, 2008.

[20] P.J. Blau, Friction microprobe investigation of particle layer effects on sliding friction. Wear, 162-164, 102-109, 1993.

[21] M. Godet, The third body approach: A mechanical view of wear. Wear, 100, 437-452, 1984.

[22] N. Fillot, I. Iordanoff, Y. Berthier, Wear modeling and the third body concept. Wear, 262, 949-957, 2007.

[23] J.W. Hall, K.L. Smith, L. Titus-Glover, J. Wambold, T.J. Yager, Z. Rado, Guide for Pavement Friction. NCHRP Web-Only Document, 108 (http://onlinepubs.trb.org/onlinepubs/nchrp/nchrp_w108.pdf), 2009.

[24] ISO 25178-2:2012. Geometrical Product Specifications (GPS) – Surface texture: Areal, Part 1: Terms, definitions and surface texture parameters, 2012.

[25] S. Descartes, C. Desrayaud and Y. Berthier, Experimental identification and characterization of the effects of contaminants in the wheel-rail contact. Proc. IMechE Part F: J. Rail and Rapid Transit, 222, 207-216, 2008.

[26] O. Arias-Cuevas, Z. Li, R. Lewis and E.A. Gallardo-Hernandez, Rolling-sliding laboratory tests of friction modifiers in dry and wet wheel-rail contacts. Wear, 268, 543-551, 2010.

[27] J. Vaze and F.H.S. Chiew, Experimental study of pollutant accumulation on an urban road surface. Urban Water, 4, 379-389, 2002.

[28] A. Deletic, D.W. Orr, Pollution build-up on road surfaces. J. Environmental Engineering, 131(1), 49-59, 2005.

[29] C.G. Giles, B.E. Sabey and K.H.F. Cardew, Development and performance of the portable skid-resistance tester. Road research technical paper, n° 66, Road Research Laboratory, 1964.

[30] EN 13036-4: 2009, Method for measurement of slip/skid resistance of surface – Part 4: the Pendulum test, 2009.

[31] ISO 48:2010, Rubber, vulcanized or thermoplastic – Determination of hardness (Hardness between 10 IRHD and 100 IRHD), 2010.

[32] R. Danzl, F. Helmli and S. Scherer, Focus variation – A robust technology for high resolution optical 3D surface metrology. J. Mechanical Engineering, 57(3), 245-256, 2011.

[33] C. Voivret, F. Radjaï, J.Y. Delenne and M.S. El Youssoufi, Space-filling properties of polydisperse granular media. Physical Review, E 76, 021301, 2007.

[34] K.A. Grosch, The relation between the friction and visco-elastic properties of rubber, Proceedings of the Royal Society of London, Series A, Mathematical and Physical Sciences, 274(1356), 21-39, 1963.

[35] P.S.M. Dougherty, R. Pudjoprawoto and C.F. Higgs, An investigation of the wear mechanism leading to self-replenishing transfer films. Wear, 272, 122-132, 2011.